J BONE ONCOL 49 (2024) 100641

Contents lists available at ScienceDirect

Journal of Bone Oncology

journal homepage: www.elsevier.com/locate/jbo

Bone density measurement in patients with spinal metastatic tumors using chest quantitative CT deep learning model

Zhi Wang [a], Yiyun Tan [a], Kaibin Zeng [a], Hao Tan [a], Pingsen Xiao [a], Guanghui Su [b,*]

[a] Department of Orthopedics, Changsha Traditional Chinese Medicine Hospital, Changsha 410002, China
[b] Department of Orthopedics, Affiliated Hengyang Hospital, Hunan Normal University (Hengyang Central Hospital), Hengyang, Hunan 421001, China

HIGHLIGHTS

- Developed 3DResUNet model for predicting vertebral vBMD from QCT scans in spinal metastasis patients.
- The model showed strong predictive performance, with Spearman correlations of 0.923 and 0.918 for vBMD.
- Achieved AUC of 0.977 (training) and 0.966 (test) for automated osteoporosis diagnosis and screening.
- Facilitates osteoporosis screening using QCT scans, especially where DXA is unavailable in clinical practice.
- Highlights bone density's role in predicting fracture risk in metastatic spinal tumor patients with deformities.

ARTICLE INFO

Keywords:
Quantitative computed tomography
Spinal metastatic tumors
Deep learning
Deep red
Volumetric bone mineral density
Bone mineral content

ABSTRACT

Objective: This study aims to develop a deep learning model using the 3DResUNet architecture to predict vertebral volumetric bone mineral density (vBMD) from Quantitative Computed Tomography (QCT) scans in patients with spinal metastatic tumors, enhancing osteoporosis screening capabilities.
Methods: 749 patients with spinal metastatic tumors underwent QCT vertebral vBMD measurements. The dataset was randomly split into training (599 cases) and test sets (150 cases). The 3DResUNet model was trained for vBMD classification and prediction using QCT images processed with automated bone segmentation and ROI extraction.
Results: The deep learning model demonstrated strong performance with Spearman correlation coefficients of 0.923 (training set) and 0.918 (test set) between predicted and QCT-measured vBMD values. Bland-Altman analysis showed a slight bias of −1.42 mg/cm^3 (training set) and −1.14 mg/cm^3 (test set) between the model predictions and QCT measurements. The model achieved an area under the curve (AUC) of 0.977 (training set) and 0.966 (test set) for diagnosing Osteoporosis based on vBMD.
Conclusion: The developed deep learning model using 3DResUNet effectively predicts vertebral vBMD from QCT scans in patients with spinal metastatic tumors. It provides accurate and automated vBMD measurements, potentially facilitating widespread osteoporosis screening in clinical practice, mainly where DXA availability is limited.

1. Introduction

According to statistics, there are over one million new cancer patients in the United States each year, with 77 % being breast, prostate, or lung cancer [1]. Among all cancer patients, approximately 50–85 % will develop bone metastases, with the spine being the most common site of bone metastases due to its unique anatomical location and blood supply characteristics [2]. In recent years, advancements in the treatment of malignant tumors have significantly extended the survival period of cancer patients. Consequently, an increasing number of patients with malignant tumors seek orthopedic consultation due to clinical manifestations of spinal metastatic tumors during their treatment. Statistics show that more than 30 % of patients with bone metastases require conservative or surgical treatment due to pathological fractures [3,4]. The one-year survival rate for patients with spinal metastatic tumors is approximately 83.3 % for prostate cancer patients, 77.7 % for breast

* Corresponding author.
E-mail address: g0708520s@163.com (G. Su).

https://doi.org/10.1016/j.jbo.2024.100641
Received 25 June 2024; Received in revised form 25 September 2024; Accepted 26 September 2024
Available online 9 October 2024

cancer patients, 51.2 % for kidney cancer patients, 21.7 % for lung cancer patients, and 0 % for stomach cancer patients [5].

In patients with metastatic spinal tumors, lesions often invade the middle column structure of the spine, particularly the posterior aspect of the vertebral body and the pedicles, making pathological fractures and secondary deformities more likely. Clinically, this can result in severe pain and symptoms of spinal cord nerve compression [6]. The lumbar spine is the most commonly affected site of metastatic spinal tumors, followed by the thoracic and cervical spine [7]. However, thoracic lesions are most likely to be accompanied by spinal cord nerve compression due to the unique anatomical features of the thoracic spine, such as a relatively narrow spinal canal, specific blood supply, lack of collateral circulation, and the propensity for kyphotic deformities following thoracic vertebral involvement [8,9]. Statistics indicate that among patients with metastatic spinal tumors accompanied by symptoms of nerve compression, approximately 70 % originate from thoracic lesions, while cervical and lumbar lesions account for 15 % each [7]. (Fig. 1).

Bone density measurement is currently one of the most essential methods for predicting fracture risk from imaging studies. It encompasses all techniques that can quantitatively measure bone mass. Various bone density measurement techniques are commonly used in clinical practice. These include conventional X-rays, X-ray absorptiometry, single-energy and dual-energy X-ray absorptiometry, quantitative computed tomography (QCT), quantitative ultrasound, and quantitative magnetic resonance imaging [10,11]. Bone densitometry, such as single-energy or dual-energy X-ray absorptiometry, measures areal bone density rather than actual volumetric bone density. Traditionally, we refer to bone mass as mineral density or mineral content. Areal density quantification is influenced by changes in bone volume, commonly occurring during bone growth and maturation. Only bone densitometry that measures volumetric density, such as quantitative computed tomography, can reflect the actual density of bone material.

QCT is currently the only method capable of measuring three-dimensional bone density and separately quantifying cortical and trabecular Bone. It is most commonly used for measuring vertebral bone density. During scanning, phantoms with different density gradients embedded in resin, typically hydroxyapatite, are placed alongside the patient's lumbar region for density comparison. Numerous studies have demonstrated a significant independent positive correlation between bone density and the mechanical strength per unit volume of Bone, making it a good indicator of mechanical strength or load-bearing capacity. However, the overall load-bearing capacity of the bone structure is also closely related to the shape of the Bone, the direction and manner of loading, and other factors. Compared to the irregular shapes of the weight-bearing parts of limb bones, the shape of vertebral bodies is relatively regular, the direction of external forces is relatively singular, and the distribution of bone density in standard or osteoporotic vertebral bodies is relatively uniform. Therefore, bone density measurements alone can adequately reflect the mechanical strength of the entire spine. Additionally, due to its large surface area and active metabolism, trabecular Bone has an eightfold higher turnover rate than cortical Bone. As a result, it can more accurately and quickly reflect changes in bone mass, and the relatively higher content of trabecular Bone within vertebral bodies allows for a good distinction between cortical and trabecular Bone.

Fig. 1. 3D Modeling of Thoracic Spine.

Both DXA and QCT, despite being the most commonly used methods for measuring bone mineral density, have specific hardware and software requirements and entail additional radiation and costs. Low-dose chest CT (LDCT) for health check-ups or other indications can assess volumetric bone mineral density (vBMD), and recent studies have shown the role of LDCT combined with QCT vertebral bone density measurements in Osteoporosis screening [12,13]. However, QCT requires manual delineation of regions of interest (ROI) on the workstation, which is time-consuming and labor-intensive. Recently, advancements in artificial intelligence (AI) in medical imaging have provided new opportunities for BMD measurements. Previous studies have shown that deep learning models can predict lumbar vBMD from QCT, correlating well with DXA measurements [14]. This study aims to build a deep-learning model based on 3DResUNet to predict vertebral vBMD from QCT and evaluate the model's performance in diagnosing Osteoporosis in patients with spinal metastatic tumors.

2. Material and methods

2.1. Case data

The case group included patients admitted to our two hospitals between 2013 and 2023 with spinal metastatic tumors and vertebral fractures. Diagnostic criteria include a more than 15 % decrease in vertebral height on the coronal or sagittal plane compared to the adjacent normal vertebrae. All subjects were initially diagnosed with spinal metastatic tumors with lesions limited to the thoracolumbar spine. Patients with cervical or sacral metastases, those who underwent chemotherapy or radiotherapy, or those who had open surgery or vertebroplasty were excluded.

Inclusion criteria: 1. Age $\geq$ 35 years. 2. Underwent QCT vertebral vBMD measurement. Exclusion criteria: 1. Poor image quality. 2. Recent intravenous contrast injection. 3. History of spinal surgery, severe fractures in the measurement area, spinal deformities, or implants. 4. Any condition affecting the spine, such as metabolic bone diseases. 5. QCT report with L1/L2 vertebral measurement value ratio exceeding three standard deviations (SD).

A total of 749 patients (462 males, 287 females, aged 35–82 years, mean age 56 $\pm$ 9 years) were included in the study. The patients were randomly assigned to the training set (599 cases) and the test set (150 cases) in an 8:2 ratio.

2.2. Data Collection

This study used the GE Optima CT680 model to scan from the lung apex to the L2 vertebra. Scanning parameters were: tube voltage 120 kV,

automatic milliampere technology, pitch 1.75:1, scanning field of view (SFOV) 500 mm, bed height 135 mm; reconstruction method: matrix 512 × 512, algorithm: LUNG, slice thickness 1.25 mm, and slice interval 1.25 mm. The new equipment was only put into use in 2018, and I don't know the specific models of the previous ones.

2.3. DXA

In recent years, DXA has been widely used to measure human BMD and BMC. International medical organizations have recognized it as the gold standard for bone density measurement, and It has become one of the most widely used methods for assessing BMD. The value of BMD can effectively reflect the bone mineral content within the human body. Based on this value, it can be determined whether osteoporosis treatment is needed, and preventive measures can be taken in advance to reduce the likelihood of fractures. Given that human bones attenuate and absorb X-rays of different energies to varying degrees, in the actual measurement process, the X-ray tube emits rays that are filtered via K-edge absorption, splitting them into two distinct energy levels. When X-rays pass through human tissues, they experience attenuation. The extent of this attenuation increases with higher bone mineral content. The BMC and BMD of specific areas can be obtained using this principle. Since bone tissue absorbs high-energy rays more than soft tissue and soft tissue absorbs low-energy rays more than bone tissue, different tissues' differences in attenuation and absorption by different rays are utilized. Combined with specially designed phantoms, the computer calculates the Bone and soft tissue in the measured area. By subtracting, the corresponding bone mineral content of the area is obtained. In theory, DXA can scan all body parts. However, the anteroposterior lumbar spine and hip are the most frequently employed areas for measurements, known for their accuracy within an error range of less than 1.0 %. Other areas, such as the hand, the radius, and the ulna, can also be scanned. Compared with other early methods, this method has a broader application range, significantly improved measurement accuracy and precision, and a relatively high safety factor for the operator.

2.4. QCT

Strictly speaking, other measurement methods do not measure accurate volumetric content. Instead, it reflects the combined density of trabecular and cortical Bone, providing a two-dimensional distribution of bone density throughout the human body. QCT is a bone density measurement method proposed in 1982 by Drs. Genant and Cann from the Department of Radiology at the University of California, San Francisco. It uses CT scanners for bone density measurements [15].

The advantage of QCT lies in its use of three-dimensional imaging, which provides high sensitivity and accuracy. This method can assess the combined density of trabecular and cortical Bone and the individual densities of trabecular and cortical Bone. The QCT method currently used in clinical practice refers explicitly to the quantitative measurement of bone density based on CT images.

The QCT bone density measurement method works based on bone minerals' high attenuation rate of X-rays. The differences in CT values of bone tissues in CT images are mainly due to differences in mineral content. Materials with absorption and attenuation properties similar to bone minerals (commonly disodium hydrogen phosphate or hydroxyapatite) are used to create phantoms of known densities. These phantoms are scanned simultaneously with the target human body part. The scanned images are segmented to isolate the region of interest, and the CT values of this region are recorded. Based on the density-to-CT value conversion relationship obtained from the phantom, the CT values of the bone tissue region are converted into bone density. Since the phantom's known density is volumetric, the converted bone density is the volumetric density we need.

The following linear relationship can represent the relationship between bone density and CT value:

$$BMD = a \times CT_{value} + b \tag{1}$$

When performing QCT measurements, a phantom of known density is scanned along with the examination area in the CT machine. Image segmentation is performed on different density calibration regions to obtain the CT values of these regions. Regression analysis is then applied to these regions' CT value distribution curve to fit a standard distribution curve. The mathematical expectation of this curve is taken as the average CT value of the calibration region. These average CT values are then substituted into the linear regression model. The formulas for calculating the slope a and intercept b in the linear relationship are as follows:

$$a = \frac{\sum_{i=1}^{n}(H_i - \overline{H})(D_i - \overline{D})}{\sum_{i=1}^{n}(H_i - \overline{H})^2} \tag{2}$$

$$b = \overline{D} - a \times \overline{H} \tag{3}$$

Where D represents the bone density value of the calibration phantom, $\overline{H}$ represents the CT value of the corresponding part of the phantom image, and I represents different calibration regions. Fig. 2 shows the least squares fitting curve. The figure shows that the values of a and b are 1.8220 and 4.471, respectively. Therefore, the linear relationship between bone density and CT value can be expressed as:

$$BMD = 1.7755 \times CT_{value} - 4.465 \tag{4}$$

This linear relationship helps convert CT values obtained from QCT scans into bone density values, providing a quantitative measure of bone density based on CT imaging.

2.5. This study uses the QCT measurement method

Through experiments, Koch et al. [16]demonstrated that both DXA and QCT are effective in measuring bone density. By comparing these measurements with the ash weight and ash weight density of vertebrae after ashing, they proved that QCT measurements of trabecular bone density are closer to ash weight density. Węgierska et al. [17]compared the diagnostic value of DXA and QCT in detecting Osteoporosis in elderly patients with rheumatoid arthritis, and their studies demonstrated that QCT exhibits a superior detection rate for Osteoporosis compared to DXA.

Among these bone density measurement methods, QCT is unique in its ability to measure trabecular and cortical bone density selectively. Additionally, QCT cannot be affected by factors such as the patient's

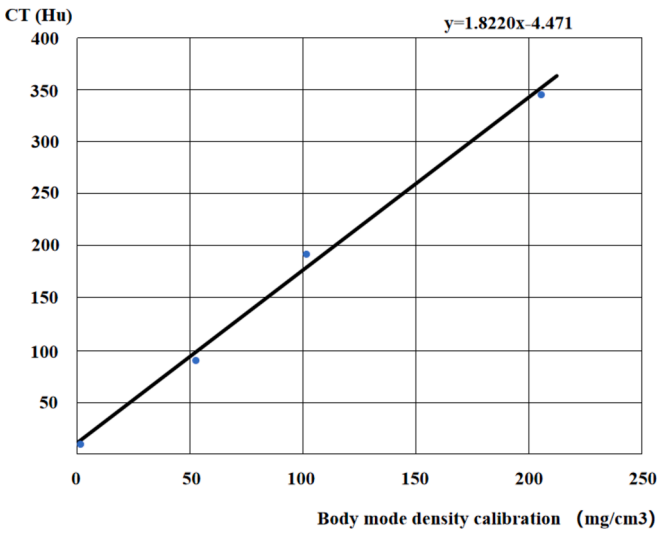

Fig. 2. Linear Relationship Fitting Curve.

height and weight. During the measurement process, the influence of surrounding factors can be eliminated, and the accuracy of the measurement results is also very high.

In summary, compared to DXA, QCT has better sensitivity and specificity in bone density measurement, and its results are more accurate. Therefore, this paper uses quantitative CT to measure the bone density of the segmented results.

2.6. QCT post-processing and BMD measurement

All CT images were transferred to the QCTPro Model 4 post-processing workstation (Mindways Software, Inc., USA) for BMD assessment. Trabecular Bone in the T12 to L2 vertebrae was measured using thoracic CT images, while lumbar and abdominal CT images were used for measurements from the L1 to L3 vertebrae. ROIs were identified at the central position of the vertebral bodies, and the average value was recorded as the patient's BMD. Diagnostic criteria followed guidelines from the International Society for Clinical Densitometry (ISCD) and the American College of Radiology (ACR). According to these standards, a trabecular bone BMD less than 80 mg/cm3 indicates Osteoporosis, BMD between 80 mg/cm3 and 120 mg/cm3 indicates low bone mass, and BMD exceeding 120 mg/cm3 indicates average bone mass. This study classified BMD into two categories: cases with normal BMD were labeled 0, and cases with low bone mass and Osteoporosis were labeled 1.

2.7. Deep learning data preparation

In this study, a deep-learning neural network for BMD binary classification and BMD value prediction was developed based on 3DResU-Net. All data were input into the Deep Red platform for vertebral segmentation, and 3 mm erosion of trabeculae was performed in the X, Y, and Z directions to obtain ROI. The ROI-related data was processed to create a paired list comprising original image paths, class labels, and ROI details. For the BMD classification model, five-fold cross-validation was employed for data partitioning. Meanwhile, the BMD value regression model utilized random grouping, dividing the dataset into a training set (n = 599) and a test set (n = 150) with an 8:2 ratio. The neural network accepted the original images as single-channel inputs and sampled around the ROI area as indicated by the ROI information. Data augmentation techniques like rotation and translation were applied to enhance the diversity of training samples. The preprocessing steps involved resampling, cropping, and normalizing the data using parameters such as crop_size, spacing, and crop_normalizers (Fig. 3).

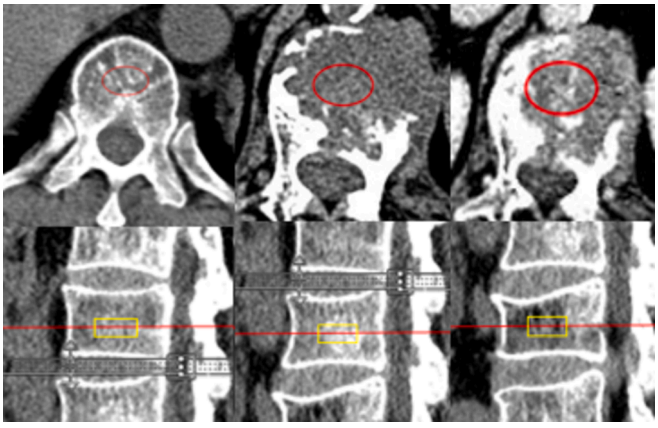

Fig. 3. Example of ROI Selection on Vertebral Image. The red ellipse represents the ROI cross-section. The ROI is located at the center of the vertebral body, excluding the cortex, to avoid bone islands and the area of the posterior vertebral venous plexus.

2.8. BMD classification model construction

The preprocessed samples were fed into the Deep Red 3DResUNet model for training. The loss function was used to evaluate the loss during the training process. With continuous iterative training, the network loss gradually decreased. The model was automatically saved every 100 training iterations, and the saved models were tested using the test set samples. This testing provided the predicted categories and prediction probabilities for each test sample. The network training was concluded once the network loss decreased to a sufficiently low level (Fig. 4).

Calculate the Mean Absolute Error (MAE), Root Mean Square Error (RMSE), and Pearson correlation coefficient between the predicted BMD values and the actual valid values for each model in a series of models. Select the optimal model based on these metrics and evaluate the optimal model using an independent test set.

3. Results

3.1. Measurement result

The QCT method was used to calculate the bone density of the cropped regions. The measurement results include cortical bone density, trabecular bone density, and the combined density of cortical and trabecular Bone, with units in mg/cm^3. Due to the large number of images, only a portion of the measurement results are listed in the Table 1 below for reference.

It is known that individual factors, environmental factors, and the measuring instrument's limitations influence bone density measurements and the diagnosis of Osteoporosis. Variations in height, weight, upbringing environment, and physical activity levels among individuals contribute to differences in bone density values. Additionally, bone mass accrual rates vary with age, meaning different individuals experience bone quality changes at different rates over time. Therefore, when conducting bone density measurements, it is crucial to consider these factors and their potential impact on measurement results.

3.2. AI model measurement results

For the analysis and measurement, the central layers of selected vertebrae are chosen (two complete vertebrae within the T12-L2 range, specifically L1 and L2). Some of the QCT and AI model measurement images are shown in Fig. 5 below.

Spearman correlation coefficients (Fig. 6a and 6b) show a positive correlation between the bone density values output by the AI model and those measured by QCT in the training set ($r = 0.923$, $P < 0.001$) and the test set ($r = 0.918$, $P < 0.001$). The within-group correlation coefficients (95 % confidence interval) are 0.937 (0.943–0.950) in the training set and 0.936 (0.937–0.951) in the test set.

Bland-Altman analysis (Fig. 6c and 6d) indicates the method differences between the AI model and QCT measurements in the training set have a bias of −1.42 (−21.81 to 19.06) mg/cm^3, with 0.043 % of points outside the 95 % Limits of Agreement (LoA). In the test set, the bias is −1.14 (−21.42 to 19.06) mg/cm^3, with 0.048 % of points outside the 95 % LoA. This suggests good agreement between the two methods.

ROC curve analysis results in the training set shows that the AI model's output for bone density diagnosis of Osteoporosis has an AUC of 0.977 (95 % CI: 0.970–0.984), while in the test set, the AUC is 0.966 (95 % CI: 0.944–0.988). Sensitivity is 41.2 %, specificity is 100 %, accuracy is 93.9 %, positive predictive value is 100 %, and negative predictive value is 93.7 % (Fig. 6e and 6f).

4. Analysis and discussion

Studies indicate that malignant tumor patients may experience tumor-related hypercalcemia, tumor-induced hypophosphatemia, and osteomalacia [18]. Epidemiological research also shows that bone

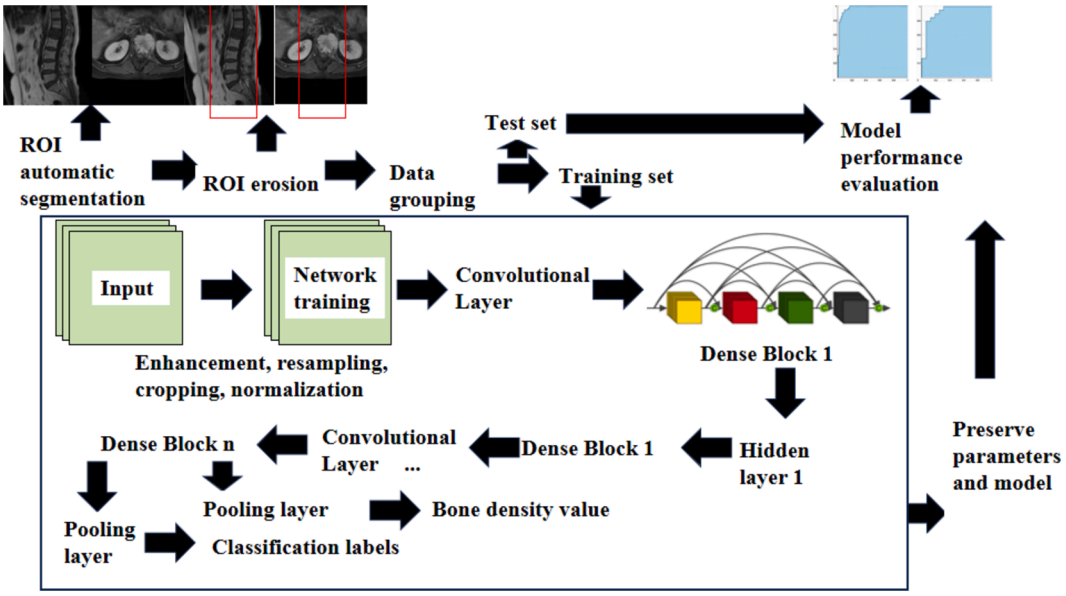

Fig. 4. Experimental Workflow.

Table 1
Partial Bone Density Measurement Results.

No.	Cortical Bone (mg/cm^3)	Trabecular Bone (mg/cm^3)	Total (mg/cm^3)
1	547.023	196.214	743.237
2	428.538	240.691	669.230
3	444.307	235.728	680.035
4	580.505	226.324	806.830
5	470.637	260.048	730.685
6	480.001	214.238	694.238

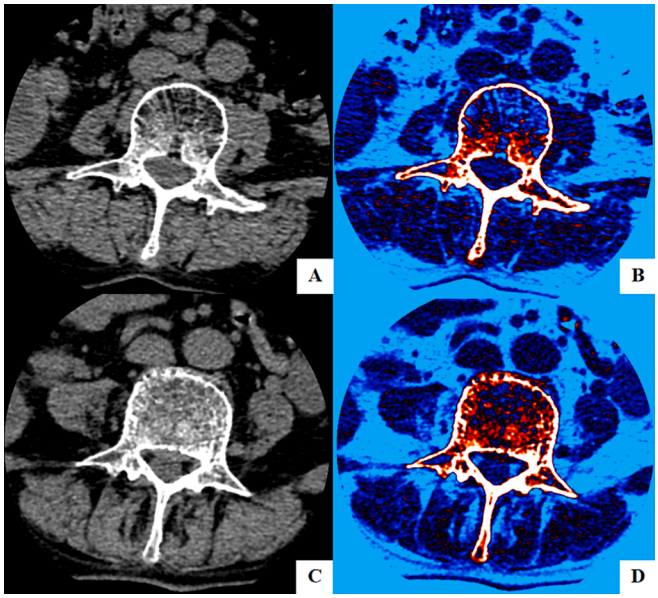

Fig. 5. (A) QCT lumbar vertebra L1 bone density measurement. (B) Model measurement of L1 bone density for the same ROI. (C) QCT measurement of lumbar vertebra L2 bone density. (D) Model measurement of L2 bone density for the same ROI.

density in tumor patients is significantly lower than in normal controls [19]. The relationship between human bone metabolism and bone fragility is closely linked, with bone density being an objective indicator widely used clinically to assess bone metabolism. Therefore, it is worth exploring whether bone density is associated with pathological vertebral fractures in metastatic spinal tumors. Using multifactorial logistic regression adjusted for gender and age, patients with low bone density have a 2.35 times higher risk of fractures compared to those with high bone density. Kanis J A et al. [20] integrated bone density indicators into an assessment model to construct a "fracture risk value" indicator for predicting fracture risk, achieving good sensitivity, specificity, and accuracy at a critical point on the ROC curve. These findings suggest that lumbar spine bone density may be related to vertebral fractures in metastatic spinal tumors, making it a promising objective measurement in predictive models.

DXA and QCT are the main methods for measuring bone density. QCT uses specialized phantoms and software to measure volumetric bone density of trabecular Bone unaffected by skeletal volume, morphology, or spinal degenerative changes, thus offering higher accuracy than DXA. However, QCT requires manual delineation of ROI, which is time-consuming and operator-dependent with inconsistent inter-operator reliability, necessitating frequent professional quality control. Using deep learning models for automatic ROI delineation helps overcome errors associated with manual operations, significantly reducing labor costs and saving time while ensuring measurement reproducibility. This model can integrate routine osteoporosis screening into patient QCT examinations without additional radiation exposure or costs.

Some studies [21] have explored the possibility of estimating BMD from CT values, reporting correlation coefficients ranging from 0.399 to 0.891. Most studies are still based on lumbar spine CT scans [22], with limited research on low-dose chest CT scans. Kaesmacher et al. [23] explored calibration phantom-based (including synchronous and asynchronous methods) and non-phantom-based (based on internal tissue calibration) possibilities, proposing formulas based on internal tissue calibration. Trabecular Bone lacks clear boundaries, making direct annotation segmentation during extraction impractical. The model developed in this study starts from automated bone segmentation, vertebral localization, cortical bone removal, and internal tissue calibration, ultimately achieving fully automated BMD output.

Further optimization and adjustment of the model are needed in

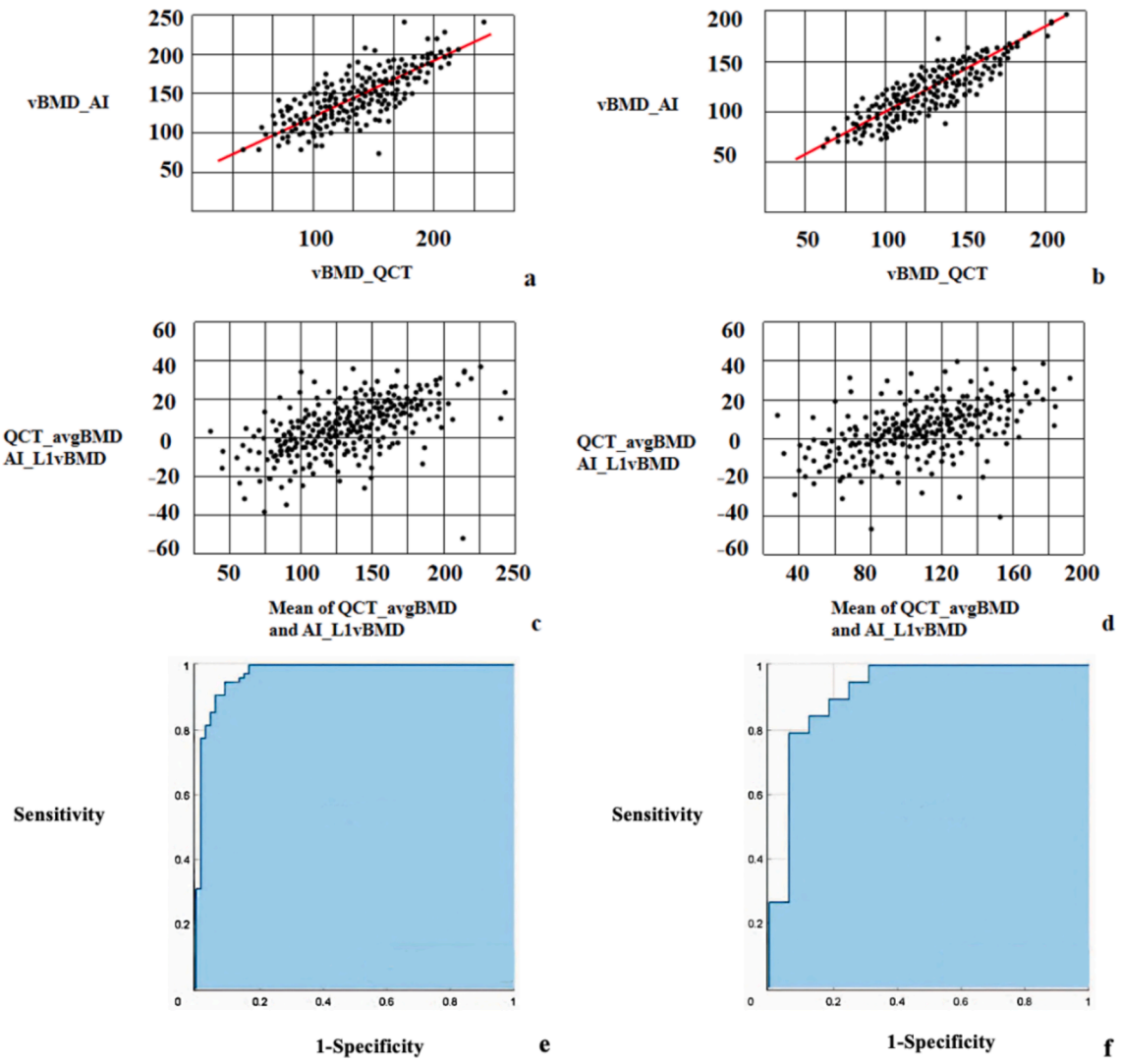

Fig. 6. (a): In the training set, there is a positive correlation between the bone density values measured by the AI model and those measured by QCT ($r = 0.923$, $P < 0.001$). (b): In the test set, there is a positive correlation between the bone density values measured by the AI model and those measured by QCT ($r = 0.918$, $P < 0.001$). (c): Bland-Altman analysis in the training set shows that the difference between the AI model and QCT bone density measurements is −1.42 (−21.81 to 19.06) mg/cm3. (d): Bland-Altman analysis in the test set shows that the difference between the AI model and QCT bone density measurements is −1.14 (−21.42 to 19.06) mg/cm3. (e): ROC curve analysis in the training set for the AI model's bone density measurements diagnosing Osteoporosis (vBMD < 80 mg/cm3) shows an AUC of 0.977. (f): ROC curve analysis in the test set for the AI model's bone density measurements diagnosing Osteoporosis (vBMD < 80 mg/cm^3) shows an AUC of 0.966.

subsequent patient studies. ICC and Bland-Altman analyses indicate high consistency between the AI model and QCT measurements of bone density. The model demonstrates high positive and negative predictive values and accuracy, meeting the demand for opportunistic osteoporosis screening in physical examinations.

This study has several limitations: (1) It is a retrospective single-center study, and the next step involves further validation of AI model consistency with QCT measurements and diagnostic efficacy for Osteoporosis in multicenter large-sample data. (2) The AI model cannot yet predict some extreme conditions, such as vertebral morphological variations, severe degenerative changes in the lumbar spine, or thin subcutaneous fat. (3) This study uses QCT measurements as the reference standard, which may introduce errors, necessitating further verification of QCT-delineated ROI and phantom calibration. Future research using deep learning models is expected to assist in quantitative analysis of the intra-abdominal fat area and other indicators, exploring more correlations between imaging and clinical information to improve predictive efficacy.

5. Conclusion

Based on the above, this study developed an automated bone density measurement model for patients with vertebral metastatic tumors using the 3DResUNet method based on QCT. It predicts vBMD from QCT scans and compares it with QCT measurement results. This approach eliminates the need for additional equipment, notable phantoms, and complex quality control processes, and it relies on something other than radiologists' experience. The research results demonstrate that this model exhibits high consistency with QCT measurements of bone density and possesses diagnostic solid efficacy. Therefore, this method can expand osteoporosis screening among populations, particularly in regions or countries with limited DXA. It holds significant importance for opportunistic screening of vertebral metastatic tumor patients.

CRediT authorship contribution statement

Zhi Wang: Writing – original draft, Validation, Resources, Methodology, Funding acquisition. **Yiyun Tan:** Writing – review & editing, Validation, Supervision. **Kaibin Zeng:** Resources, Data curation. **Hao**

Tan: Visualization, Resources, Data curation, Conceptualization. **Pingsen Xiao:** Investigation, Formal analysis, Conceptualization. **Guanghui Su:** Writing – review & editing, Visualization, Validation, Project administration, Funding acquisition.

Declaration of competing interest

The authors declare that they have no known competing financial interests or personal relationships that could have appeared to influence the work reported in this paper.

References

[1] Jemal A, Siegel R, Ward E, et al. Cancer statistics, 2009. CA: Cancer J. Clin, 2009, 59(4): 225-249.
[2] C.S.B. Galasko, The anatomy and pathways of skeletal metastases, Bone Metastases (1981) 49–63.
[3] J.A. Ortiz Gómez, The incidence of vertebral body metastases, Int. Orthop. 19 (1995) 309–311.
[4] J. Walls, N. Bundred, A. Howell, Hypercalcemia and bone resorption in malignancy, Clin. Orthopaed. Related Res. 312 (1995) 51–63.
[5] H. Tatsui, T. Onomura, S. Morishita, et al., Survival rates of patients with metastatic spinal cancer after scintigraphic detection of abnormal radioactive accumulation, Spine 21 (18) (1996) 2143–2148.
[6] A. Pr, Do metastases in vertebrae begin in the body or the pedicles? Imaging study in 45 patients, AJR 158 (1992) 1275–1279.
[7] J. Brihaye, P. Ectors, M. Lemort, et al., The management of spinal epidural metastases, Adv. Tech. Stand. Neurosurg. (1988) 121–176.
[8] M. Nottebaert, A.R. Von Hochstetter, G.U. Exner, et al., Metastatic carcinoma of the spine: a study of 92 cases, Int. Orthop. 11 (1987) 345–348.
[9] Urist M R, Gurvey M S, Fareed D O. Long-term observations on aged women with pathologic osteoporosis. Osteoporosis. New York: Grune and Stratton, 1970: 3-37.
[10] D. Marshall, O. Johnell, H. Wedel, Meta-analysis of how well measures of bone mineral density predict occurrence of osteoporotic fractures, BMJ 312 (7041) (1996) 1254–1259.
[11] O. Johnell, J.A. Kanis, A. Oden, et al., Predictive value of BMD for hip and other fractures (Journal of Bone and Mineral Research (2005) 20, (1185–1194)), J. Bone Miner. Res. 22 (5) (2007) 774.
[12] Y. Wu, Y. Jiang, X. Han, et al., Application of low-tube current with iterative model reconstruction on Philips Brilliance iCT Elite FHD in the accuracy of spinal QCT using a European spine phantom, Quant. Imaging Med. Surg. 8 (1) (2018) 32.
[13] X. Cheng, K. Zhao, X. Zha, et al., Opportunistic screening using low-dose CT and the prevalence of osteoporosis in China: a nationwide, multicenter study, J. Bone Miner. Res. 36 (3) (2020) 427–435.
[14] K. Yasaka, H. Akai, A. Kunimatsu, et al., Prediction of bone mineral density from computed tomography: application of deep learning with a convolutional neural network, Eur. Radiol. 30 (2020) 3549–3557.
[15] H.K. Genant, C.E. Cann, B. Ettinger, et al., Quantitative computed tomography of vertebral spongiosa: a sensitive method for detecting early bone loss after oophorectomy, Ann. Intern. Med. 97 (5) (1982) 699–705.
[16] V. Koch, N.G. Hokamp, M.H. Albrecht, et al., Accuracy and precision of volumetric bone mineral density assessment using dual-source dual-energy versus quantitative CT: a phantom study, Eur. Radiol. Expe. 5 (2021) 1–10.
[17] M. Węgierska, M. Dura, E. Blumfield, et al., Osteoporosis diagnostics in patients with rheumatoid arthritis, Reumatologia/rheumatology 54 (1) (2016) 29–34.
[18] T. Ohnishi, E. Takeda, S. Yogita, et al., Effects of alendronate on bone metastases and hypercalcemia after surgery for hepatocellular carcinoma, Jpn. J. Clin. Oncol. 30 (9) (2000) 410–413.
[19] A. Berruti, L. Dogliotti, C. Terrone, et al., Changes in bone mineral density, lean body mass and fat content as measured by dual energy x-ray absorptiometry in patients with prostate cancer without apparent bone metastases given androgen deprivation therapy, J. Urol. 167 (6) (2002) 2361–2367.
[20] J.A. Kanis, F. Borgstrom, C. De Laet, et al., Assessment of fracture risk, Osteoporos. Int. 16 (2005) 581–589.
[21] E.B. Gausden, B.U. Nwachukwu, J.J. Schreiber, et al., Opportunistic use of CT imaging for osteoporosis screening and bone density assessment: a qualitative systematic review, JBJS 99 (18) (2017) 1580–1590.
[22] L. Liu, M. Si, H. Ma, et al., A hierarchical opportunistic screening model for osteoporosis using machine learning applied to clinical data and CT images, BMC Bioinf. 23 (1) (2022) 63.
[23] J. Kaesmacher, H. Liebl, T. Baum, et al., Bone mineral density estimations from routine multidetector computed tomography: a comparative study of contrast and calibration effects, J. Comput. Assist. Tomogr. 41 (2) (2017) 217–223.